Terra Nova

WILEY

Terra Nova

RESEARCH ARTICLE

Syn-Collisional Origin of Yidun Arc-Like Magmas and Northern Provenance of Songpan-Ganzi Turbidites (Eastern Tibet)

Xiumian Hu[1] | Dingjun Wen[2] | Yingdi Pan[1] | Eduardo Garzanti[3] | Tao Deng[1] | Xiaolong Dong[1] | Anlin Ma[1] | Zhuohao Zhao[1]

[1]State Key Laboratory for Critical Earth Material and Mineral Deposits, School of Earth Sciences and Engineering, Nanjing University, Nanjing, China | [2]School of Earth and Planetary Sciences, East China University of Technology, Nanchang, China | [3]Laboratory for Provenance Studies, Department of Earth and Environmental Sciences, University of Milano-Bicocca, Milano, Italy

Correspondence: Xiumian Hu (huxm@nju.edu.cn)

Received: 27 June 2025 | **Revised:** 6 December 2025 | **Accepted:** 19 December 2025

Keywords: eastern Tibet plateau | oceanic subduction | paleo-Tethys | provenance analysis | syn-collisional magmatism | Triassic | Yidun arc

ABSTRACT

The accurate identification of ancient magmatic arcs through igneous characteristics is crucial for reliable paleogeodynamic reconstructions. This study evaluates the widely accepted Yidun arc hypothesis in the eastern Tibetan Plateau. Upper Triassic (235–200 Ma) high-K metaluminous, arc-type rocks in the Zhongza terrane show crustal reworking based on Hf isotopes. Lower–Middle Triassic turbidites intruded by these igneous rocks share detrital modes and detrital-zircon U–Pb ages with Songpan-Ganzi turbidites, supported by southward paleocurrents, indicating a shared northern Kunlun-Qinling source. Field evidence confirms that turbidites in both the Zhongza and Songpan-Ganzi terranes predate the widespread Upper Triassic arc-like igneous rocks in Zhongza. These rocks formed via syn-collisional, not oceanic subduction, magmatism, challenging the arc model. This highlights the importance of detailed geological analysis before interpreting arc-like magmatism and inferring subduction polarity in ancient orogens.

1 | Introduction

The ~500 km-long and ~60–180 km-wide Zhongza terrane (historically called Yidun or Zhongdian) in the eastern Tibetan Plateau is separated from the Qiangtang Block by the Jinshajiang suture zone to the west and from the Songpan-Ganzi terrane by the Ganzi-Litang suture zone in the east (Pan et al. 1997; Wang et al. 2000) (Figure 1a–c). The eastern side of the Zhongza terrane is lined by a discontinuous belt of igneous rocks covering > 7500 km^2 (Figure 1c,d) and yielding arc-like geochemistry (e.g., negative Nb-Ta anomalies, high alkali metals, high FeO/MgO and low MgO and TiO_2). Reid, Wilson, Phillips et al. (2005), Reid, Wilson and Liu (2005) and Reid et al. (2007) investigated the age, tectonic deformation and cooling history of those magmatic rocks and formally referred to them as the Yidun Arc, a proposal widely accepted in the literature thereafter. The presence of the 'Yidun arc' was later used to argue for the eastward subduction of the Jinshajiang Ocean (e.g., Pullen et al. 2008; Ding et al. 2013) or for the westward subduction of a Ganzi-Litang Ocean (Reid, Wilson, and Liu 2005). The economically important porphyry Cu-Mo-Au deposits of the Sanjiang mineralization belt are considered closely related to 'Yidun arc' magmatism (Hou 1993; Deng et al. 2022). Magmatic rocks with arc-like geochemistry, however, can also form in the syn-collisional stage (e.g., Periadriatic plutons in the European Alps or Linzizong Group in the Gangdese arc of southern Tibet; Ji et al. 2019; Zhu et al. 2023).

To test whether the arc-like Zhongza magmatic rocks are the direct product of oceanic subduction, we carried out field investigations to better characterise their geodynamic setting and

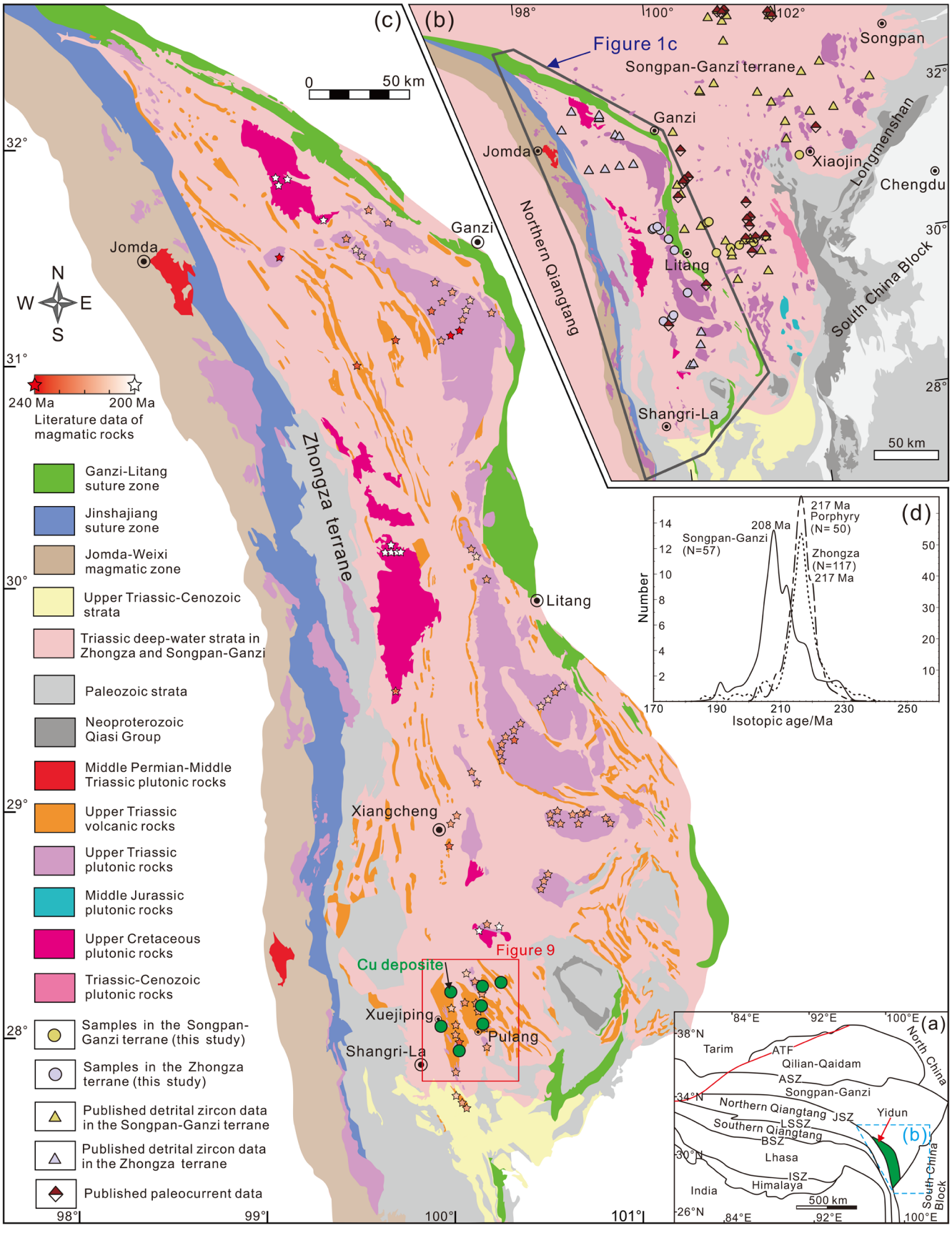

FIGURE 1 | Legend on next page.

FIGURE 1 | (a) Zhongza terrane in the eastern Tibetan Plateau. ATF, Altyn-Tagh Fault. Suture zones: ASZ, A'nyemaqen; JSZ, Jinshajiang; LSSZ, Longmucuo-Shuanghu; BSZ, Bangong-Nujiang; ISZ, Indus-Yarlung. (b) Simplified geological map of Zhongza terrane, study area and location of sandstone and paleocurrent samples discussed in text. (c) Map showing the spatial and temporal distribution of Upper Triassic intrusive and volcanic rocks (modified after Zhan et al. 2021). (d) Probability density plot of zircon U–Pb ages of magmatic rocks in Zhongza and Songpan-Ganzi terranes (Table S1). [Colour figure can be viewed at wileyonlinelibrary.com]

geological relationship with the intruded sedimentary rocks. The tectonic setting and sediment provenance of Triassic turbidites were investigated by sedimentary petrography and U–Pb ages of detrital zircons. To better understand the paleogeodynamic framework of the Zhongza terrane as a whole, we compiled mineralogical and geochemical data on Upper Triassic magmatic rocks in both Zhongza and Songpan-Ganzi terranes for comparison.

2 | Geological Background

The Jinshajiang Ocean developed between the Zhongza and Qiangtang terranes during the middle to late Palaeozoic, as evidenced by 382–264 Ma gabbro and diabase intrusions and Devonian–Early Permian radiolarian cherts (Zi et al. 2013) (Figure 2a). Westward subduction from the late Early Permian to the Late Permian produced a suite of volcanic rocks until oceanic closure by Early Triassic–early Middle Triassic time. Closure timing is constrained stratigraphically by the unconformity at the base of the Lower–Middle Triassic Malasongduo felsic volcaniclastic succession (252–242 Ma; Wang et al. 2024), by peak metamorphic ages of 248–244 Ma in eclogites (Tang et al. 2025), and by 247–240 Ma syn-collisional to post-collisional magmatism (Reid et al. 2007; Zi et al. 2013). The Ganzi-Litang deep-marine domain opened by the Devonian–Carboniferous as indicated by radiolarian biostratigraphy (Figure 2a), with sea-floor spreading possibly initiating locally in the Permian (Yu et al. 2024). As a Permian rift, the Ganzi-Litang zone formed, which did not develop into a full ocean (sensu Liu and Wang 2023) as indicated by the lack of mature oceanic crust. Paleomagnetic results on Upper Triassic volcanic rocks in the Zhongza terrane broadly constrain the closure of the Ganzi-Litang proto-ocean as a branch of Paleo-Tethys to the early Late Triassic (Cao et al. 2025; Hu et al. 2025).

The Zhongza terrane includes Palaeozoic clastic and carbonate rocks locally intercalated with volcanic rocks, and Lower to Middle Triassic deep-marine siliciclastic rocks of the Yidun Group in the east (Figure 3a–e). The stratigraphy and detrital-zircon U–Pb ages show affinity with the western margins of both South China (Figure 2b,c) and North Qiangtang blocks. The Middle to Upper Permian volcano-sedimentary sequences of the Zhongza terrane are similar to the Emeishan flood basalts (Yang et al. 2024). The 10–15 km-thick coeval turbiditic succession of the Xikang Group characterises the Songpan-Ganzi terrane (Weislogel et al. 2006, 2010; Ding et al. 2013; Jian et al. 2019).

3 | Materials and Methods

Lower to Middle Triassic sandstone samples (12 from the Zhongza terrane and 9 from the southeastern Songpan-Ganzi terrane) were selected for petrographic analysis. At least 400 grains were counted in each sample following the Gazzi-Dickinson point-counting method (Ingersoll et al. 1984). The counting results were classified and plotted following Garzanti (2019). Two Triassic sandstones from the Zhongza terrane were analysed for U–Pb detrital-zircon ages (Figure 1); for provenance analysis and tectonic interpretation, the results were compared with published geochronological and geochemical data from magmatic and sedimentary rocks. A detailed description of the adopted analytical methods and the complete dataset is provided as Supporting Information.

4 | Results

4.1 | Yidun Magmatic Rocks

The Upper Triassic magmatic rocks exposed in the Zhongza terrane include both plutonic and volcanic rocks (Figures 1b, 3f–l and 4d–i; Table 1; Table S1). The intrusive complex, represented by the Ganzi and Daocheng batholiths and by ore-bearing granitic rocks near Shangri La (Figure 3), mainly consists of tonalite, granodiorite and porphyritic granite locally containing mafic enclaves. Zircon U–Pb dating indicates crystallisation ages from 228 to 202 Ma (Figure S1, Figure 5). A minor number of zircon crystals or parts of crystals yielding ages ranging from 2627 to 365 Ma are considered as inherited (Reid et al. 2007). Variable SiO_2 (52–76 wt%) and K_2O (1.4–9.6 wt%) concentrations and low A/CNK ($Al_2O_3/[CaO+Na_2O+K_2O]$) and A/NK ($Al_2O_3/[Na_2O+K_2O]$) ratios (Table S3) indicate high-K calc-alkaline affinity (Figure 5). The enrichment in large-ion lithophile elements (Rb, Th, K) and depletion in high field strength elements (Nb, Ta, Ti) are consistent with arc-like trace-element characteristics.

The Upper Triassic volcanic rocks, mainly exposed on the western side of the magmatic domain and interlayered with sedimentary rocks, include basalt, andesite and dacite (Wang et al. 2011; Leng et al. 2014). These volcanic rocks span a narrower time interval than intrusive rocks (231–212 Ma; Wang et al. 2011), exhibit low SiO_2 (45–66 wt%), variable K_2O (0–4.9 wt%) and total alkalis (K_2O+Na_2O up to 9.3 wt%), indicating calc-alkaline affinity (Figure 5). Plutonic rocks in the Zhongza terrane yielded negative zircon $\varepsilon_{Hf}(t)$ (from −15.5 to −2.0) and whole-rock $\varepsilon_{Nd}(t)$ values (from −9.5 to −1.5) (Figure 5). In contrast, volcanic rocks and ore-bearing porphyry display variable zircon $\varepsilon_{Hf}(t)$ values (from −1.4 to +11.3 and from −5.6 to +7.3, respectively) and whole-rock $\varepsilon_{Nd}(t)$ (from −4.2 to +6.3 and from −4.9 to +1.5, respectively) (Table 1 and Table S3 and Figure 5).

4.2 | Provenance of Deep-Marine Triassic Turbidites

Lower-Middle Triassic turbidites in both Zhongza ($n=12$) and Songpan-Ganzi ($n=9$) terranes are mostly feldspatho-litho-quartzose and litho-quartzose sandstones (average Q:F:L = 67 ± 13:10 ± 5:23 ± 9; Figure 6a; Table S4) with felsic

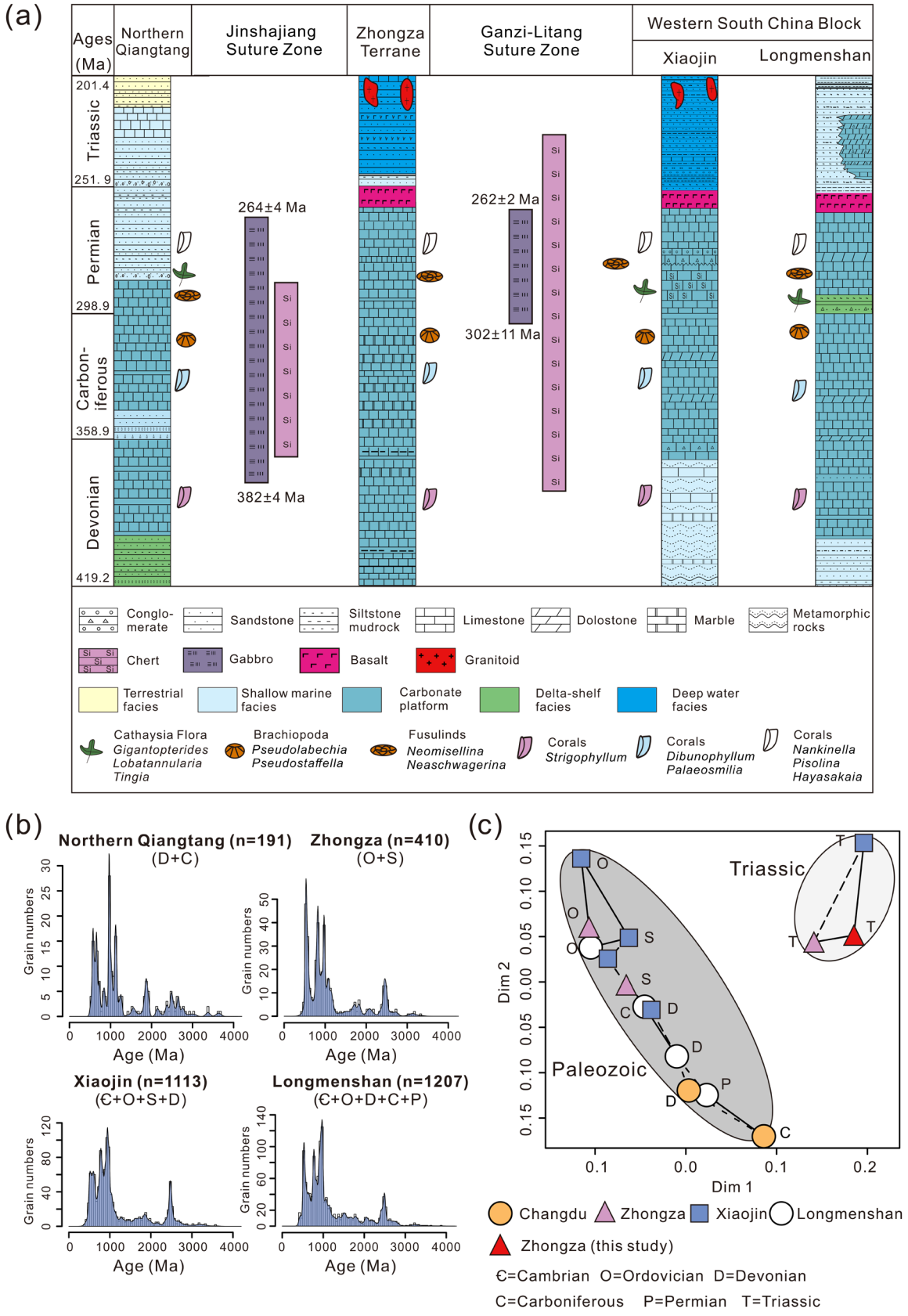

FIGURE 2 | (a) Comparison of compiled stratigraphic columns for Zhongza and Northern Qiangtang terranes (Tian et al. 2023) with Xiaojin and Longmenshan areas of the western margin of South China Block (Liu and Wang 2023). (b) Palaeozoic detrital zircon kernel density estimation (KDE) plot. (c) Multi-dimensional scaling (MDS) plot of Palaeozoic and Triassic detrital zircons. Closest and second-closest neighbours are linked by solid and dashed lines, respectively. Data sources for Palaeozoic detrital zircons, Cathaysia flora, corals, fusulinds and brachiopods are listed in Table S2. [Colour figure can be viewed at wileyonlinelibrary.com]

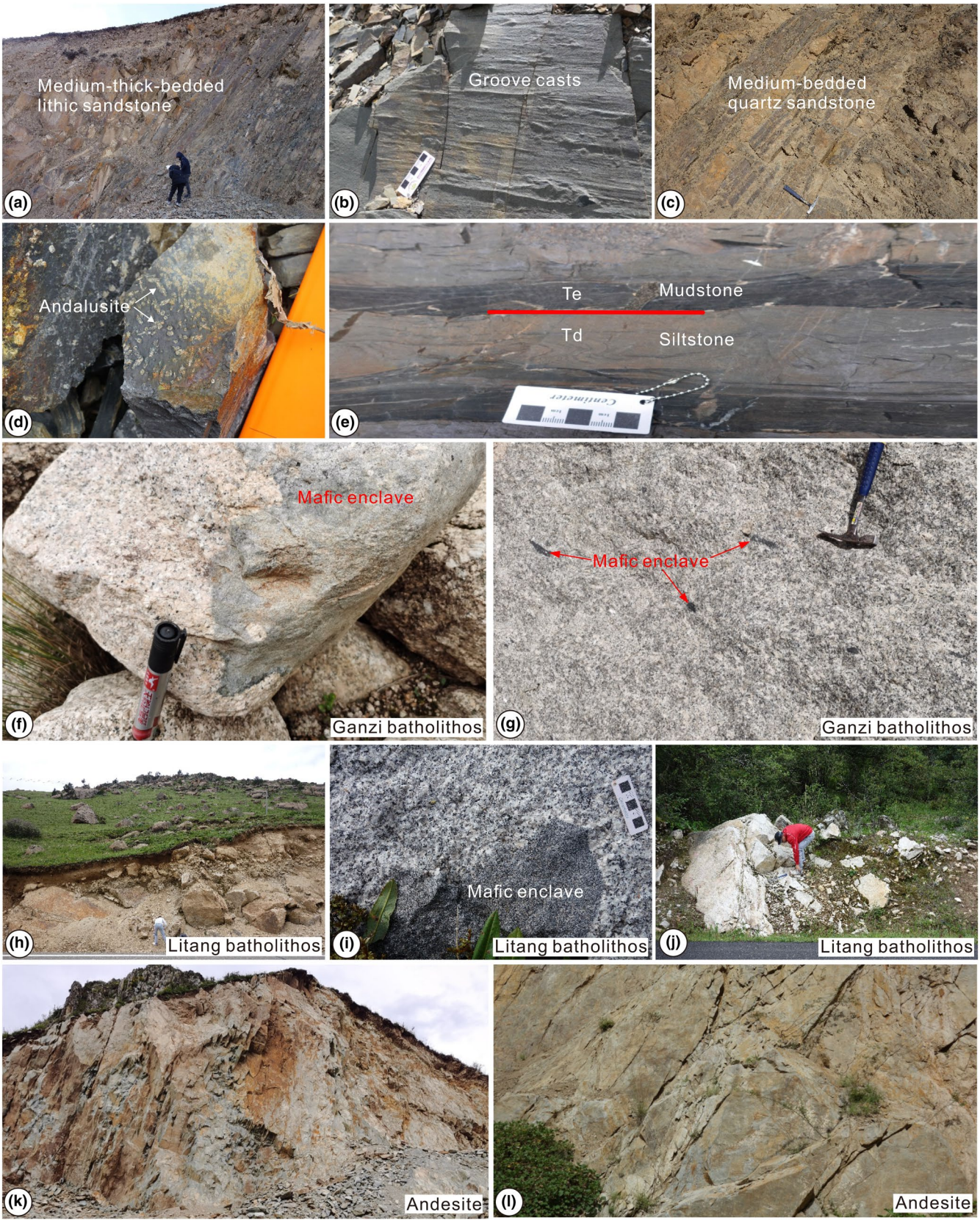

FIGURE 3 | Field photographs of Triassic turbidites and magmatic rocks from the Songpan-Ganzi and Zhongza terranes. (a) Medium-thick bedded litho-quartzose sandstone of Songpan-Ganzi terrane (GPS: 30.1654° N, 100.5449° E). (b) Groove casts. (c) Medium-bedded litho-quartzose sandstone of Zhongza terrane (GPS: 30.3761° N 99.7951° E). (d) Andalusite hornfels in wall rock of Upper Triassic granite in Zhongza terrane (GPS: 29.1433° N, 99.9295° E). (e) Incomplete Bouma sequence in Triassic turbidites of Zhongza terrane. Field photographs of Ganzi (f, g) and Litang batholiths (h–j). Field photographs of volcanic rocks in the Zhongza terrane (k, l). [Colour figure can be viewed at wileyonlinelibrary.com]

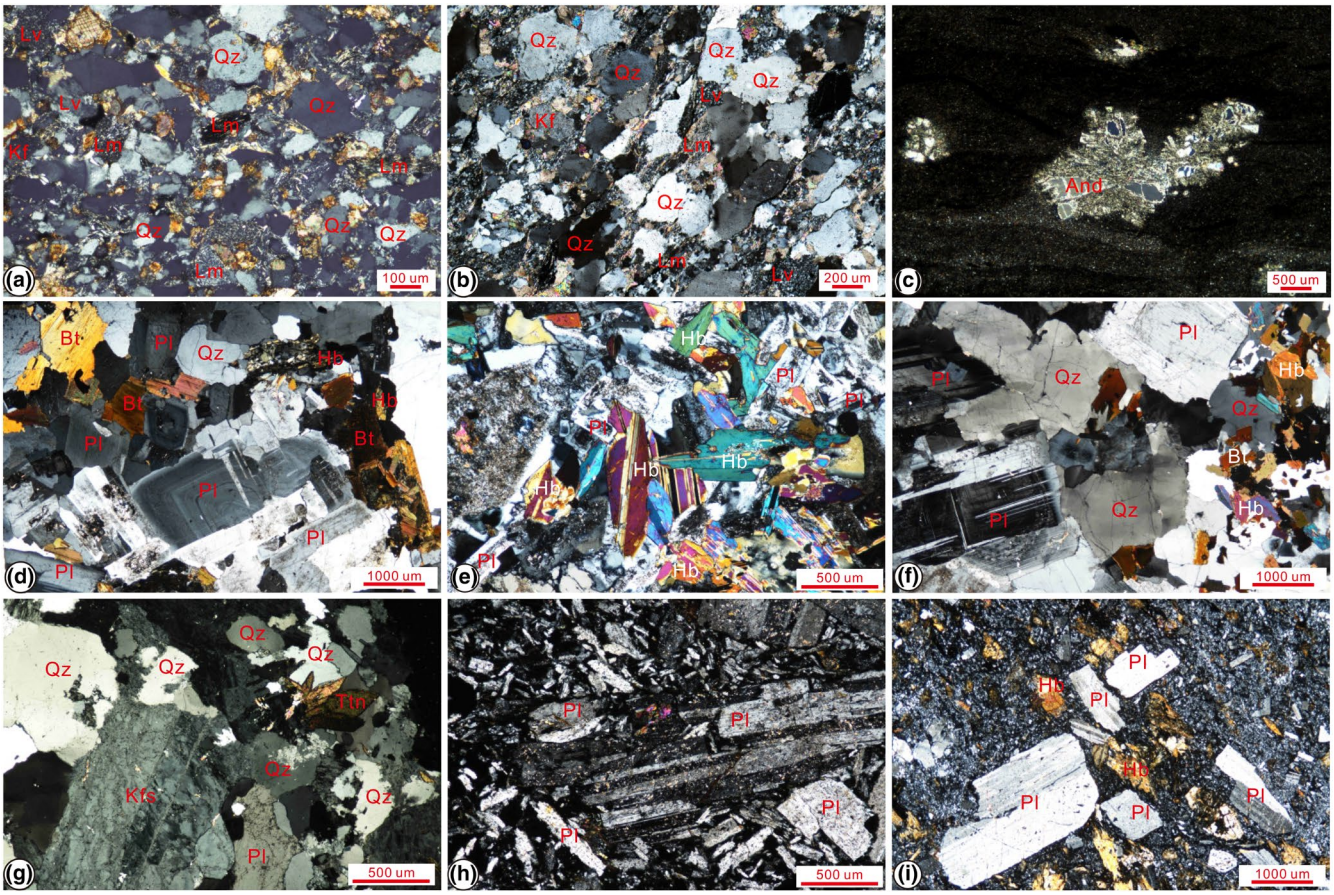

FIGURE 4 | Photomicrographs of sedimentary, metamorphic and magmatic rocks in Songpan-Ganzi and Zhongza terranes. Triassic litho-quartzose sandstones in Songpan-Ganzi (a) and Zhongza (b) terranes. (c) Andalusite hornfel in the wall rock of Upper Triassic granite in the Zhongza terrane. (d–g) Upper Triassic granites in Ganzi and Litang batholiths. (h-i) Upper Triassic volcanic rocks in the Zhongza terrane. Hb, hornblende; Pl, plagioclase; Kfs, K-feldspar; And, andalusite; Qz, quartz; Lv, felsic igneous lithic; Lm, metamorphic lithic. [Colour figure can be viewed at wileyonlinelibrary.com]

volcanic (average 49% ± 11%) and subordinate metamorphic lithics (slate, phyllite, minor schist; average 41% ± 15%) (Figure 6a). Detrital zircons in the Yidun Group display major U–Pb age peaks at 269, 443, 794, 967, 1878 Ma and a minor cluster around 2478Ma (Figure 6b, Figure S2; Table S5). Similar peaks at 269, 432, 782 and 1861 Ma in the Xikang Group point to the same detrital source.

The potential sources include North China, Qiangtang, South China, East Kunlun terranes and the Qinling orogen (Nie et al. 1994; Weislogel et al. 2006, 2010; Jian et al. 2019; Tang et al. 2023; Chen et al. 2023; Table S6). Major contributions from the North China Block are ruled out, because the NCB is characterised by zircon-age peaks at 1.8 and 2.5 Ga and a lack of a Neoproterozoic peak at ~970 Ma (Figure 6b, Jian et al. 2019). Moreover, sediment transport from the North China Block would have been blocked by the North Qinling orogen, reaching a paleo-elevation up to ~4000 m in the Late Triassic based on magmatic rocks' mohometers (Chen et al. 2023). Major contributions from the Qiangtang terrane are also ruled out, because the latter is characterised by a prominent Pan-African age peak at ~538 Ma lacking in Yidun and Xikang sandstones (Figure 6b).

The East Kunlun and Qinling orogens represent the most plausible sources of siliciclastic detritus by far. These orogens experienced two magmatic phases, in the early-middle Palaeozoic (460–400 Ma) and in the Middle Permian to Late Triassic (268–210 Ma) (Dong et al. 2011, 2018; Dai et al. 2013), matching zircon-age peaks in Triassic sandstones. Measurements of flute casts, ripple foresets, ripple casts and ripple bedform-dip directions were conducted at 6 localities near Songpan county, 2 localities near Xiaojin county, 20 localities near Yajiang county and 2 localities in the Zhongza terrane (Weislogel 2006; Figure S3), pointing at southward paleocurrents (Weislogel et al. 2006, 2010; Jian et al. 2019). Provenance from the north is thus indicated (Figure 6c). In the Yajiang–Xiaojin area, instead, paleocurrents mainly trend toward the northwest and southwest, plausibly reflecting large-scale clockwise crustal rotation during the Jurassic–Cenozoic as supported by paleomagnetic data showing up to ~70° of clockwise rotation of coherent blocks along the southeastern Tibetan margin (Wang et al. 2014; Li et al. 2017). The Yajiang region lies south of the Cenozoic left-lateral Xianshuihe Fault (Figure S3), suggesting that the southeastern Songpan-Ganzi region may have experienced Cenozoic southeastward extrusion and clockwise rotation after the India–Asia collision, also affecting the measured direction of Triassic paleocurrents.

5 | Discussion and Implications

No Triassic ophiolitic rocks have been identified in the Zhongza terrane. Existing ophiolites in the Jinshajiang suture zone are

TABLE 1 | Compiled zircon U–Pb ages and geochemical features of Upper Triassic magmatic rocks in Zhongza and Songpan-Ganzi terranes.

Regions	Plutons	Rock type	Age (Ma)	$\varepsilon_{Hf}(t)$	$\varepsilon_{Nd}(t)$	SiO_2 (wt.%)	K_2O (wt.%)	Na_2O (wt.%)
Songpan-Ganzi terrane	Taiyanghe	Diorite	205	−3.18 to +3.89		57.92 to 51.38	5.35 to 1.31	4.06 to 2.82
	Yanggonghai	S-type granite	221		−9.6 to −9.4	73.47 to 72.61	4.93 to 4.68	3.19 to 3.01
	Maoergai	Adakitic rock	216		−8.7 to −8.0	73.73 to 72.26	4.39 to 3.81	4.22 to 3.39
	Markam	S-type granite	188 to 153		−9.9 to −5.4	74.60 to 66.56	5.97 to 3.20	4.81 to 2.32
	Nyanbaoyeche	Granite	211		−2.72	78.16 to 74.00	6.28 to 4.87	3.47 to 3.07
	Menggu	Granite	224	−2.85 to −0.36	−6.50 to −3.84	75.99 to 67.20	5.38 to 3.55	5.12 to 2.67
	Manai	Granite	197		−7.37 to −1.63			
	Tagong	Granodiorite/MME	209 to 208	−6.9 to −1.4	−7.49 to −7.08	64.3 to 61.6	3.72 to 3.16	1.82 to 1.67
	Riluku	Monzogranite	208 to 206	−6.6 to +2.1	−5.0 to −3.4	72.65 to 68.78	5.10 to 2.33	4.21 to 3.08
	Niuxingou	Granite	215	+3.99 to +0.31	−3.59 to −0.29	74.67 to 53.70	6.35 to 3.44	4.43 to 3.11
Zhongza terrane	Cuo'a	Granodiorite/Enclave	219	−14.0 to −6.7		69.23 to 66.73	3.33 to 2.69	2.82 to 2.56
	Shaluli	Monzogranite	214	−14.3 to −6.9	−8.9 to −6.2	76.13 to 71.74	4.04 to 3.04	3.35 to 2.63
	Dongcuo	Monzogranite	220 to 217	−14.4 to −8.1	−9.5 to −6.1	73.79 to 72.41	4.88 to 4.73	2.84 to 2.70
	Dongcuo	Dioritic enclave	220	−5.6 to −2.5		64.35 to 51.47	3.08 to 0.77	3.25 to 2.32
	Maxiongou	Monzogranite	225 to 216		−6.2 to −5.7	74.75 to 73.10	4.60 to 4.45	3.41 to 3.23
	Shengmu	Granodiorite	212	−7.6 to −5.3	−7.7 to −6.4	64.52 to 61.33	3.30 to 2.26	2.89 to 2.62
	Shengmu	Enclave/Quartz diorite	217	−11.7 to −1.98	−4.9 to −1.5	60.48 to 52.74	2.58 to 1.39	3.35 to 2.37
	Citu	Granodiorite	213	−15.5 to −8.8		67.65	3.57	3.03
	Lannitang	Quartz monzonite	216		−4.0 to −2.3	64.60 to 51.56	3.00 to 2.34	5.84 to 4.02
	Pulang	Granodiorite	224 to 212	−8.6 to +1.3	−4.9 to −2.2	68.40 to 55.40	9.64 to 2.26	5.93 to 2.60
	Xuejiping	Monzonite	217 to 216	−4.4 to +6.2	−4.0 to +1.5	64.64 to 57.18	3.59 to 1.54	4.56 to 3.24
	Disuga	Quartz diorite	221 to 218	−8.4 to +7.3	−4.2 to −0.1	64.45 to 61.16	4.56 to 2.35	3.06 to 1.58
	Xiuwacu	Monzonite/Granite	221 to 214	−7.5 to +4.9	−2.2 to −0.1	75.80 to 57.65	5.99 to 3.15	3.78 to 2.56

Note: Data sources from Upper Triassic magmatic rocks in Zhongza terrane after Reid et al. (2007), Cao et al. (2016), Fang (2017), Wu et al. (2017) and Zhan et al. (2021) and in Songpan-Ganzi terrane after Roger et al. (2004), Li et al. (2007), Xiao et al. (2007), Yuan et al. (2010), Cai et al. (2009, 2010), Chen et al. (2017), Zhan et al. (2020), Qiu et al. (2024) and Yan et al. (2024).

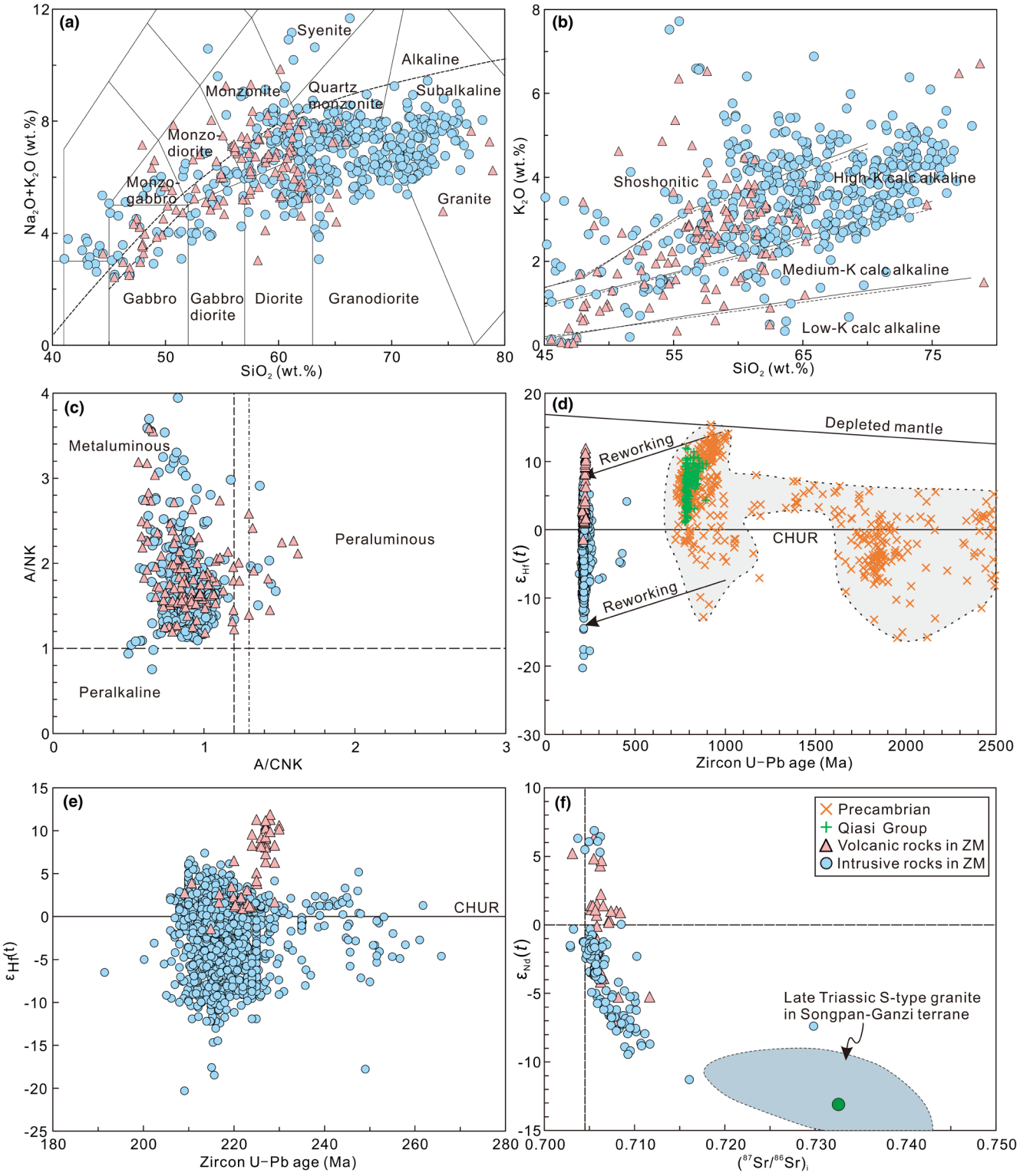

FIGURE 5 | (a) SiO_2 versus ($K_2O + Na_2O$) plot. (b) SiO_2 versus K_2O plot. (c) A/CNK versus A/NK plot. (d, e) Zircon U–Pb age versus $\varepsilon_{Hf}(t)$ plot. (f) ($^{87}Sr/^{86}Sr$) versus $\varepsilon_{Nd}(t)$ plot. Whole-rock major and trace-element, Sr-Nd isotope and zircon Lu-Hf isotope data on Upper Triassic magmatic rocks of the Zhongza terrane are listed in Table S3. [Colour figure can be viewed at wileyonlinelibrary.com]

dated as 382–264 Ma (Zi et al. 2013), pre-dating the Late Triassic magmatism.

Upper Triassic (235–200 Ma) plutonic and volcanic rocks exposed along the eastern side of the Zhongza terrane are unlikely to represent a magmatic-arc setting based on several lines of evidence. These rocks are metaluminous and high-K calc-alkaline, distinct from the medium-K calc-alkaline rocks typical of arc magmas (Figure 5; Zhu et al. 2023). Moreover, the overall enriched whole-rock Sr–Nd and zircon Hf isotopes

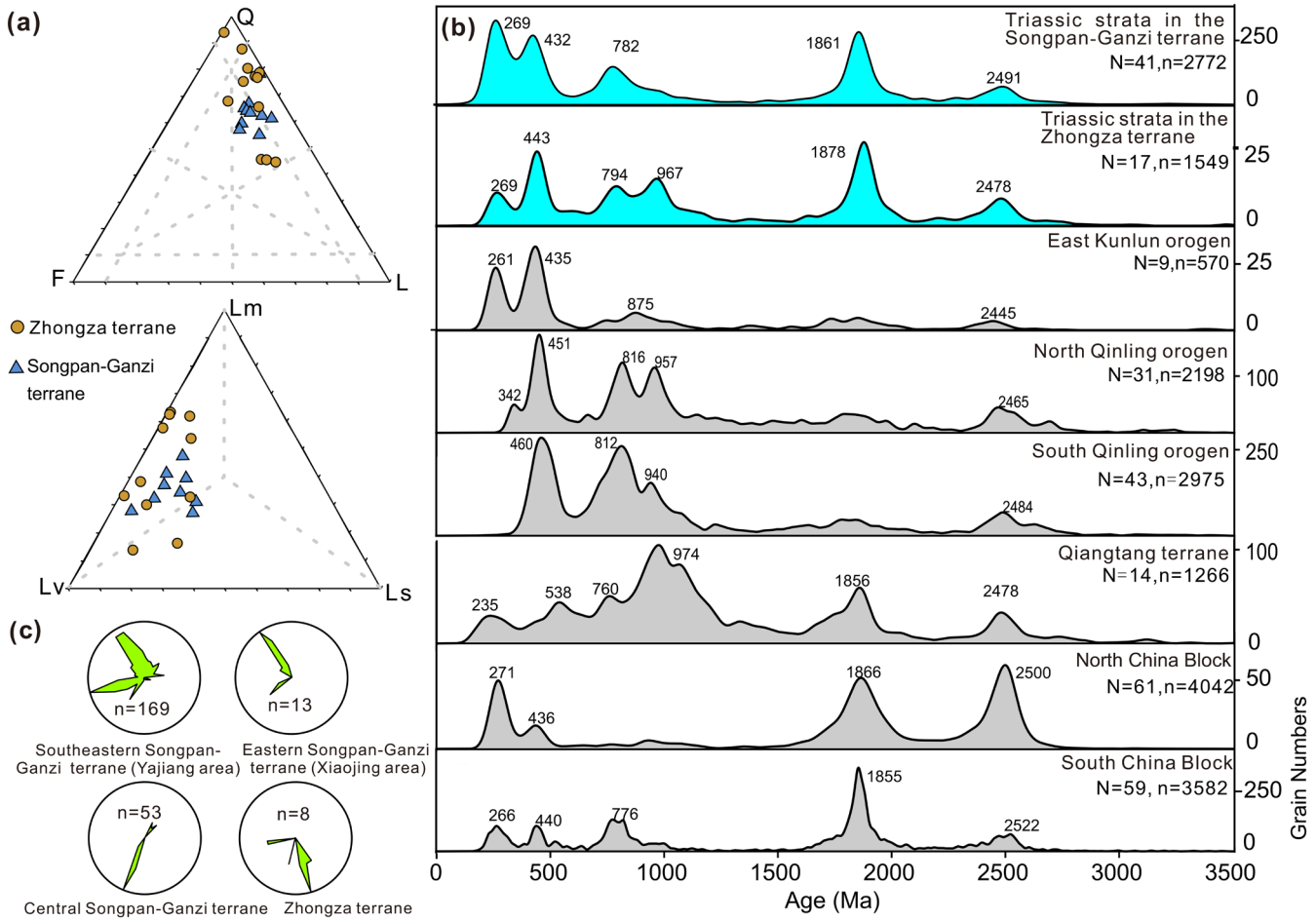

FIGURE 6 | (a) Quartz-Feldspar-Lithic and metamorphic-volcanic-sedimentary lithic plots for Triassic Yidun and Xikang turbidites. (b) U–Pb age spectra of detrital zircons in Triassic turbidites compared with potential source terranes (all KDE plots drawn with 50 Ma bandwidth). *N*, number of samples; *n*, number of zircon ages. (c) Paleocurrent data from Triassic Yidun and Xikang turbidites in Zhongza and Songpan-Ganzi terranes (from Weislogel 2006). [Colour figure can be viewed at wileyonlinelibrary.com]

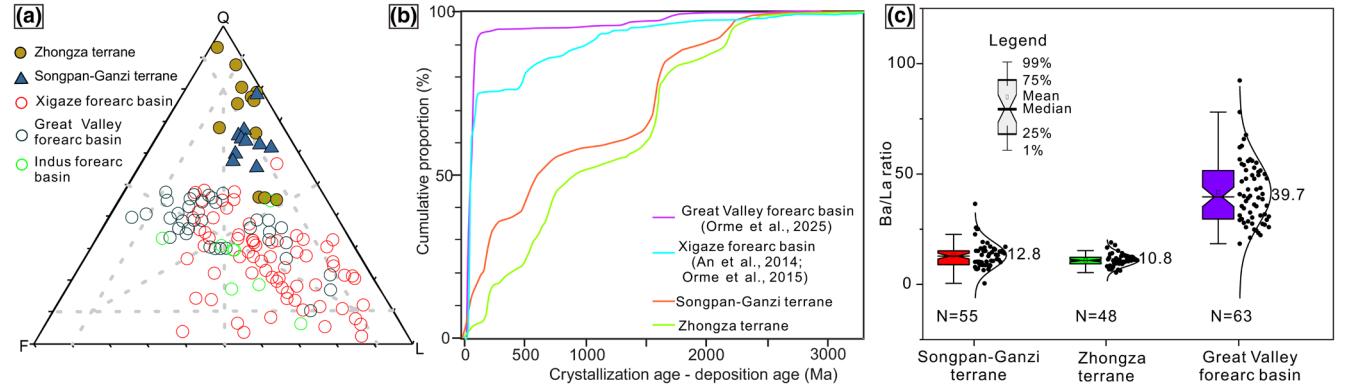

FIGURE 7 | (a) Composition of Triassic turbiditic sandstones from Songpan-Ganzi and Zhongza terranes contrasts with forearc-basin sandstones worldwide [data for Great Valley forearc basin from Gilbert and Dickinson 1970 and Ingersoll 1983; data for Xigaze forearc basin from An et al. 2014 and Orme and Laskowski 2016; data for Indus forearc basin from Garzanti and Van Haver 1988]. (b) Cumulative curves of detrital-zircon ages from Triassic turbidites compared with those in forearc basins (base diagram from Cawood et al. 2012). Data sources indicated in legend (An et al. 2014; Orme et al. 2015, 2025). (c) Box plots of whole-rock Ba/La ratios for Songpan-Ganzi and Zhongza Triassic mudrocks, compared with fine-grained clastics from the Great Valley forearc basin. Data sources: Songpan-Ganzi after Weislogel et al. (2006); Zhongza after Wang et al. (2013); Great Valley after Surpless (2015) and Orme et al. (2025). [Colour figure can be viewed at wileyonlinelibrary.com]

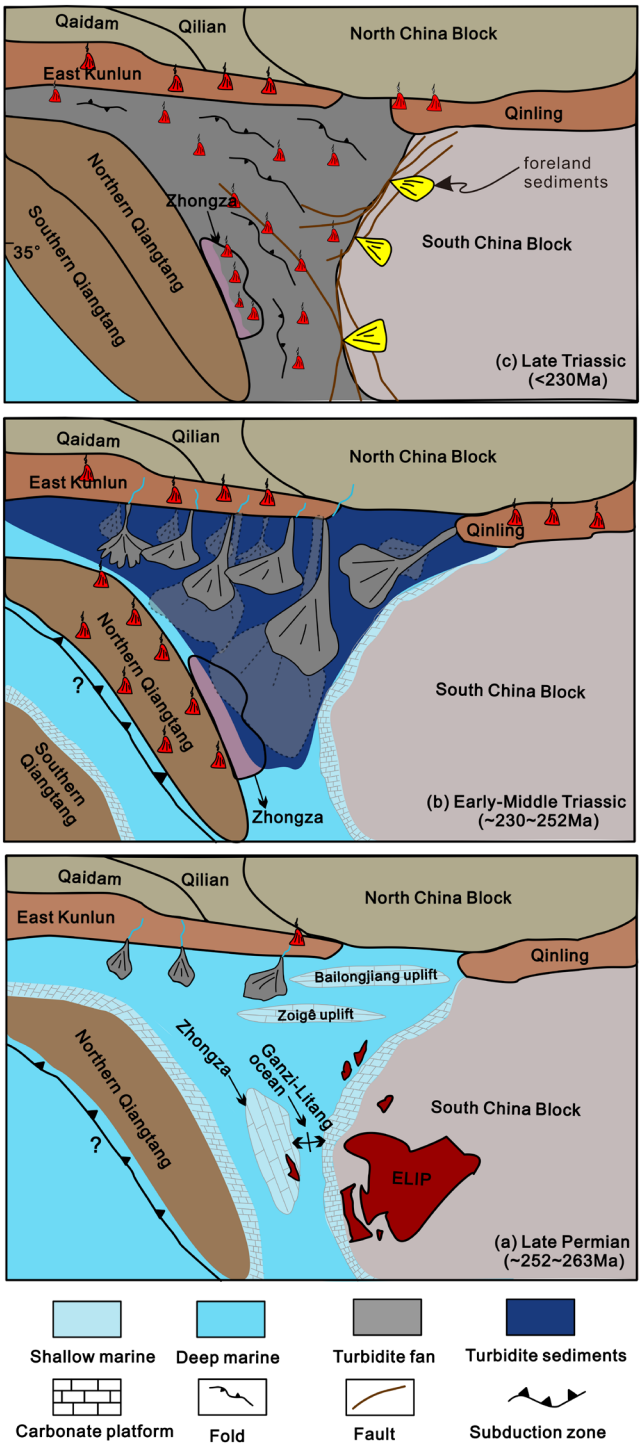

FIGURE 8 | Late Permian–Triassic evolution of Zhongza terrane. (a) Late Permian: Eruption of Emeishan Large Igneous Province (ELIP) associated with the formation of Ganzi-Litang rift. The East Kunlun orogen supplies detritus to the Songpan-Ganzi terrane. (b) Early-Middle Triassic: Jinshajiang and Ganzi-Litang rift close. Zhongza and Songpan-Ganzi terranes receive detritus from East Kunlun and Qinling orogens. (c) Late Triassic: Syn- to post-collisional magmatism and fold-thrust deformation in Zhongza and Songpan-Ganzi terranes. [Colour figure can be viewed at wileyonlinelibrary.com]

(Figure 5) indicate dominant crustal reworking, inconsistent with subduction-zone magmas (Zhu et al. 2023). It has been argued that ultramafic cumulates are representative of lower-arc crust, but cumulates contemporaneous with intermediate–felsic I-type granites have not been reported in the Zhongza terrane so far (Zhu et al. 2021).

The decisive evidence proving the syn-collisional (Zhan et al. 2021) rather than arc-related origin of this magmatic suite, however, comes from unambiguous field observations. Upper Triassic plutonic rocks display clear intrusive contacts with Lower–Middle Triassic turbidites, with a thermal metamorphic aureole characterised by growth of andalusite (Figures 3d and 4c). Such a relationship proves beyond doubt that turbidite deposition preceded by a considerable amount of time their deformation and subsequent intrusion of Upper Triassic magmatic rocks. Reid, Wilson, and Liu (2005) interpreted fold axes parallel to the Yidun magmatic belt as arc-parallel structures, but field documentation of intrusive contacts with folded turbidites proves that these folds post-date magmatism and reflect syn-collisional compression rather than arc formation (Figure 3d).

No evidence indicates that Upper Triassic magmatic rocks and Yidun turbidites are linked to an arc-trench system, or that such a system existed in the Late Triassic, a period marked instead by collision-related deformation (Xu et al. 2024). This argument is primarily supported by three key lines of evidence: (1) The feldspatho-litho-quartzose to litho-quartzose composition of Triassic sandstones, with much higher quartz content than in volcanolithic forearc-basin sandstones worldwide (Gilbert and Dickinson 1970; Ingersoll 1983), as well documented all along the Himalayan forearc basin (Garzanti and Van Haver 1988; An et al. 2014; Orme and Laskowski 2016) (Figure 7a). (2) Detrital zircons in Yidun turbidites display multiple and older age peaks rather than a dominant coeval peak as expected in arc-related basins (Cawood et al. 2012) (Figure 7b). (3) Elevated Ba/La ratios in sedimentary rocks are indicative of slab-derived fluid influence on continental arc magmatism (Solidum et al. 2003), a geochemical signal incorporated in volcano-plutonic sediments deposited in forearc or intra-arc basins. Triassic mudrocks from the Songpan-Ganzi and Zhongza terranes exhibit markedly lower Ba/La ratios (median 12.8 and 10.8, respectively) than sediments from the Great Valley forearc basin (median 39.7). This can be considered additional evidence against an arc origin of Songpan-Ganzi and Zhongza sediments (Figure 7c). These arguments indicate the Triassic sedimentary rocks are not associated with an oceanic subduction-related arc system as held by Reid, Wilson, and Liu (2005).

Pullen et al. (2008) proposed that the Yidun arc separated from the southern margin of the Kunlun-Qaidam terranes by subduction reversal during consumption of the Paleo-Tethys ocean. Geological evidence, however, indicates that the Zhongza terrane did not rift away from the Kunlun-Qaidam terranes but rather from the western margin of the South China Block, as documented by the strong Upper Palaeozoic stratigraphic affinity of both Zhongza and Songpan-Ganzi terranes with the South China Block (Figure 2). Most relevant, the Permian Emeishan Large Igneous Province is exposed both in the Zhongza terrane and along the western margin of the South China Block, suggesting that the Ganzi-Litang deep-water domain never developed into a true oceanic branch (Chang 2000; Liu and Wang 2023) but rather represents a rift that failed at the proto-oceanic stage during the Permian (Figure 8a).

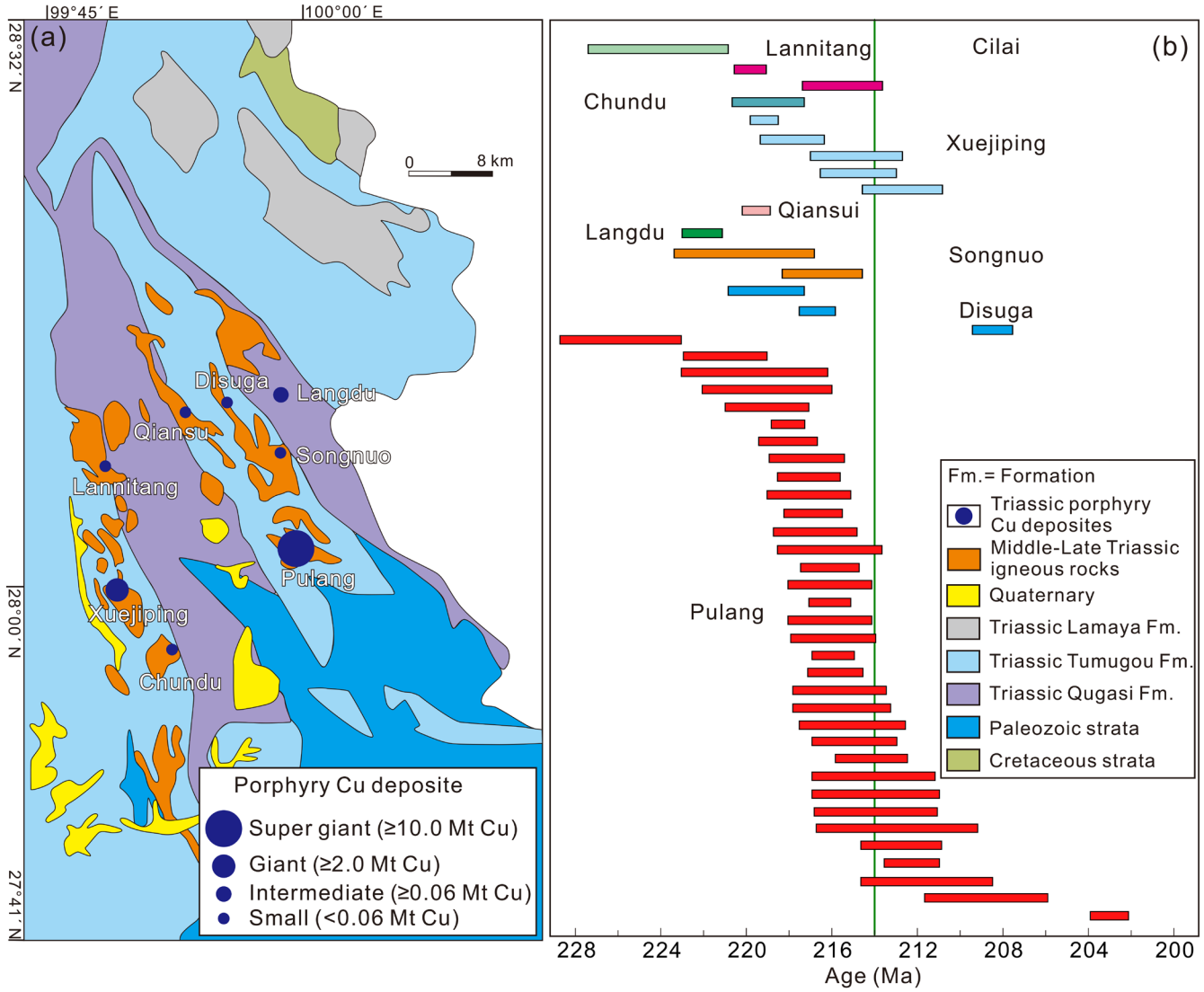

FIGURE 9 | (a) Distribution and size of porphyry copper deposits in the Pulang area. (b) Geochronology of ores in the Pulang mining area. Original data and references are provided in detail in Table S1. [Colour figure can be viewed at wileyonlinelibrary.com]

The Zhongza and Songpan-Ganzi terranes formed an integrated domain underlain by hyper-extended continental crust in the Triassic, when it was filled by Yidun and Xikang deep-sea turbidites. Both Zhongza and Songpan-Ganzi terranes were subsequently involved in collision during the Late Triassic, when they experienced contractional deformation and metamorphism associated with extensive syn-collisional magmatism (Figure 8b,c).

Syn-collisional magmatism widely occurs in other orogenic regions. Following the onset of the India-Asia continental collision dates as ~61–59 Ma (Hu et al. 2015; An et al. 2021), the Linzizong lavas were erupted parallel to the newly-formed orogenic belt (Zhu et al. 2021, 2022). Similarly, the Eocene–Oligocene (55–25 Ma) Urumieh-Dokhtar magmatic arc—originally suggested to have been produced during Neo-Tethyan oceanic subduction (Chiu et al. 2013)—developed after the onset of the Arabia-Asia continental collision, recently constrained as pre-Eocene (Sun et al. 2023). Although most igneous rocks in orogenic belts were traditionally interpreted as associated with the oceanic-subduction phase, recent stratigraphic and geochronological data indicate that a considerable part of them was instead generated shortly after the onset of continental subduction, implying that the paleogeographic and paleogeodynamic significance of orogenic magmatism needs to be revisited and carefully reassessed at the global scale.

The formation of most porphyry copper deposits worldwide is associated with hydrous, calc-alkaline to mildly alkaline, intermediate-felsic magmas with arc-like and adakitic geochemical characteristics (Richards 2009). This is also the case for the Sanjiang mineralization belt (Figure 9), but it does not prove that associated arc-like magmas were generated during oceanic subduction.

Our findings underscore the need to reassess the syn-collisional versus post-collisional setting of arc-like magmatic rocks and advocate for integrated sedimentological, petrographic and paleogeographical approaches in unravelling the complex linkage between arc-like magmatic rocks (including ore-bearing porphyry) and subduction processes.

Acknowledgements

This study was supported by the Project of Deep Earth Exploration and Mineral Resource Prospecting, National Science and Technology Major Project of China (No. 2024ZD1001103) and National Natural Science Foundation of China—Tethyan Project (Grant No. 91755209). We thank Wendong Liang and Fengting Chen for their help in the field. Thanks to Alex Pullen for constructive feedback on an earlier version of the manuscript. This work was greatly improved through insightful discussions with Academician Zhiqin Xu, Academician Fuyuan Wu, and Prof. Dicheng Zhu. We are also grateful to Editor Prof. Carlo Doglioni and an anonymous reviewer for their valuable and constructive comments.

Funding

This work was supported by the Project of Deep Earth Exploration and Mineral Resource Prospecting, National Science and Technology Major Project of China, 2024ZD1001103; National Natural Science Foundation of China - Tethyan Project, 91755209.

Conflicts of Interest

The authors declare no conflicts of interest.

Data Availability Statement

The data supporting the findings of this study are available in the Supporting Information of this article.

References

An, W., X. Hu, E. Garzanti, M. K. BouDagher-Fadel, J. Wang, and G. Sun. 2014. "Xigaze Forearc Basin Revisited (South Tibet): Provenance Changes and Origin of the Xigaze Ophiolite." *Geological Society of America Bulletin* 126: 1595–1613. https://doi.org/10.1130/B31020.1.

An, W., X. Hu, E. Garzanti, J. G. Wang, and Q. Liu. 2021. "New Precise Dating of the India-Asia Collision in the Tibetan Himalaya at 61 Ma." *Geophysical Research Letters* 48, no. 3: e2020GL090641. https://doi.org/10.1029/2020GL090641.

Cai, H. M., H. F. Zhang, and W. C. Xu. 2009. "U–pb Zircon Ages, Geochemical and Sr–Nd–hf Isotopic Compositions of Granitoids in Western Songpan–Garze Fold Belt: Petrogenesis and Implication for Tectonic Evolution." *Journal of Earth Science* 20: 681–698. https://doi.org/10.1007/s12583-009-0068-8.

Cai, H. M., H. F. Zhang, W. C. Xu, Z. L. Shi, and H. L. Yuan. 2010. "Petrogenesis of Indosinian Volcanic Rocks in Songpan–Garze Fold Belt of the Northeastern Tibetan Plateau: New Evidence for Lithospheric Delamination." *Science China. Earth Sciences* 53: 1316–1328. https://doi.org/10.1007/s11430-010-4032-0.

Cao, K., J. F. Xu, J. L. Chen, et al. 2016. "Double-Layer Structure of the Crust Beneath the Zhongdian Arc, SW China: U–pb Geochronology and hf Isotope Evidence." *Journal of Asian Earth Sciences* 115: 455–467. https://doi.org/10.1016/j.jseaes.2015.11.001.

Cao, Y., Z. Sun, H. Li, et al. 2025. "First Paleomagnetic Results from Late Triassic Volcanic Rocks of the Yidun Terrane, Eastern Tibetan Plateau: Constraints on the Closure of the Paleo-Tethys Ocean." *Geophysical Research Letters* 52, no. 20: e2025GL118769. https://doi.org/10.1029/2025GL118769.

Cawood, P. A., C. J. Hawkesworth, and B. Dhuime. 2012. "Detrital Zircon Record and Tectonic Setting." *Geology* 40, no. 10: 875–878. https://doi.org/10.1130/G32967.1.

Chang, E. Z. 2000. "Geology and Tectonics of the Songpan-Ganzi Fold Belt, Southwestern China." *International Geology Review* 42, no. 9: 813–831. https://doi.org/10.1080/00206810009465113.

Chen, G., F. Hu, A. H. Robertson, E. Garzanti, S. Zhang, and F. Y. Wu. 2023. "A Combined Methodology for Reconstructing Source-To-Sink Basin Evolution, Exemplified by the Triassic Songpan–Ganzi Basin, Central China." *Sedimentary Geology* 458: 106529. https://doi.org/10.1016/j.sedgeo.2023.106529.

Chen, Q., M. Sun, G. Zhao, et al. 2017. "Origin of the Mafic Microgranular Enclaves (MMEs) and Their Host Granitoids From the Tagong Pluton in Songpan–Ganze Terrane: An Igneous Response – The Closure of the Paleo-Tethys Ocean." *Lithos* 290: 1–17. https://doi.org/10.1016/j.lithos.2017.07.024.

Chiu, H. Y., S. L. Chung, M. H. Zarrinkoub, S. S. Mohammadi, M. M. Khatib, and Y. Iizuka. 2013. "Zircon U–pb Age Constraints From Iran on the Magmatic Evolution Related to Neotethyan Subduction and Zagros Orogeny." *Lithos* 162: 70–87. https://doi.org/10.1016/j.lithos.2013.01.006.

Dai, J., C. Wang, J. Hourigan, and M. Santosh. 2013. "Multi-Stage Tectono-Magmatic Events of the Eastern Kunlun Range, Northern Tibet: Insights From U–pb Geochronology and (U–Th)/He Thermochronology." *Tectonophysics* 599: 97–106. https://doi.org/10.1016/j.tecto.2013.04.005.

Deng, J., Q. Wang, X. Sun, et al. 2022. "Tibetan Ore Deposits: A Conjunction of Accretionary Orogeny and Continental Collision." *Earth-Science Reviews* 235: 104245. https://doi.org/10.1016/j.earscirev.2022.104245.

Ding, L., D. Yang, F. Cai, et al. 2013. "Provenance Analysis of the Mesozoic Hoh-Xil-Songpan-Ganzi Turbidites in Northern Tibet: Implications for the Tectonic Evolution of the Eastern Paleo-Tethys Ocean." *Tectonics* 32, no. 1: 34–48. https://doi.org/10.1002/tect.20013.

Dong, Y., D. He, S. Sun, et al. 2018. "Subduction and Accretionary Tectonics of the East Kunlun Orogen, Western Segment of the Central China Orogenic System." *Earth Science Reviews* 186: 231–261. https://doi.org/10.1016/j.earscirev.2017.12.006.

Dong, Y., G. Zhang, F. Neubauer, X. Liu, J. Genser, and C. Hauzenberger. 2011. "Tectonic Evolution of the Qinling Orogen, China: Review and Synthesis." *Journal of Asian Earth Sciences* 41, no. 3: 213–237. https://doi.org/10.1016/j.jseaes.2011.03.002.

Fang, X. 2017. "Petrogenesis of the Middle-Late Triassic Intermediate-Acid Intrusive Rocks in the Yidun Terrane and Its Geological Significances." Master thesis, University of Chinese Academy of Sciences, Beijing.

Garzanti, E. 2019. "Petrographic Classification of Sand and Sandstone." *Earth-Science Reviews* 192: 545–563. https://doi.org/10.1016/j.earscirev.2018.12.014.

Garzanti, E., and T. Van Haver. 1988. "The Indus Clastics: Forearc Basin Sedimentation in the Ladakh Himalaya (India)." *Sedimentary Geology* 59, no. 3–4: 237–249.

Gilbert, W. G., and W. R. Dickinson. 1970. "Stratigraphic Variations in Sandstone Petrology, Great Valley Sequence, Central California Coast." *Geological Society of America Bulletin* 81: 949–954. https://doi.org/10.1130/0016-7606(1970)81[949:SVISPG]2.0.CO;2.

Hou, Z. 1993. "Tectono-Magmatic Evolution of the Yidun Island-Arc and Geodynamic Setting of Kuroko-Type Sulfide Deposits in Sanjiang Region, China." *Resource Geology Special Issue* 17: 336–350 (in Chinese).

Hu, X., E. Garzanti, T. Moore, and I. Raffi. 2015. "Direct Stratigraphic Dating of India-Asia Collision Onset at the Selandian (Middle Paleocene, 59 ±1 Ma)." *Geology* 43, no. 10: 859–862. https://doi.org/10.1130/G36872.1.

Hu, X., A. Ma, J. Wang, et al. 2025. "The Odyssey from Marine to Continental Transition in the TibetanPlateau: A Duet of Tectonic and Sealevel Change." *Acta Sedimentologica Sinica* 43: 1569–1591. https://doi.org/10.14027/j.issn.1000-0550.2025.046. (in Chinese with English abstract.).

Ingersoll, R. V. 1983. "Petrofacies and Provenance of Late Mesozoic Forearc Basin, Northern and Central California." *AAPG Bulletin* 67:

1125–1142. https://doi.org/10.1306/03B5B5A9-16D1-11D7-8645000102C1865D.

Ingersoll, R. V., T. F. Fullard, R. L. Ford, J. P. Grimm, J. D. Pickle, and S. W. Sares. 1984. "The Effect of Grain Size on Detrital Modes: A Test of the Gazzi-Dickinson Point-Counting Method." *Journal of Sedimentary Research* 54: 103–116. https://doi.org/10.1306/212F83B9-2B24-11D7-8648000102C1865D.

Ji, W. Q., M. G. Malusà, M. Tiepolo, A. Langone, L. Zhao, and F. Y. Wu. 2019. "Synchronous Periadriatic Magmatism in the Western and Central Alps in the Absence of Slab Breakoff." *Terra Nova* 31, no. 2: 120–128. https://doi.org/10.1111/ter.12376.

Jian, X., A. Weislogel, and A. Pullen. 2019. "Triassic Sedimentary Filling and Closure of the Eastern Paleo-Tethys Ocean: New Insights From Detrital Zircon Geochronology of Songpan-Ganzi, Yidun, and West Qinling Flysch in Eastern Tibet." *Tectonics* 38, no. 2: 767–787. https://doi.org/10.1029/2018TC005300.

Leng, C. B., Q. Y. Huang, X. C. Zhang, et al. 2014. "Petrogenesis of the Late Triassic Volcanic Rocks in the Southern Yidun Arc, SW China: Constraints From the Geochronology, Geochemistry, and Sr–Nd–pb–hf Isotopes." *Lithos* 190: 363–382. https://doi.org/10.1016/j.lithos.2013.12.018.

Li, S., E. L. Advokaat, D. J. J. van Hinsbergen, M. Koymans, C. Deng, and R. Zhu. 2017. "Paleomagnetic Constraints on the Mesozoic-Cenozoic Paleolatitudinal and Rotational History of Indochina and South China: Review and Updated Kinematic Reconstruction." *Earth-Science Reviews* 171: 58–77. https://doi.org/10.1016/j.earscirev.2017.05.007.

Li, Z. C., X. Z. Pei, S. P. Ding, et al. 2007. "Zircon U–pb Dating of the Nanyili Granodiorite in the Pingwu Area, Northwestern Sichuan, and Its Geological Significance." *Geology in China* 34: 1003–1012. (in Chinese with English Abstract.).

Liu, S., and Y. Wang. 2023. "Origin of the Songpan-Garze Terrane on the Northeastern Tibetan Plateau, Eastern Segment of the Tethyan Tectonic Domain: A Middle Permian–Early Triassic Intracontinental Rifting System." *GSA Bulletin* 135: 1993–2014. https://doi.org/10.1130/B36468.1.

Nie, S., A. Yin, D. B. Rowley, and Y. Jin. 1994. "Exhumation of the Dabie Shan Ultra-High-Pressure Rocks and Accumulation of the Songpan-Ganzi Flysch Sequence, Central China." *Geology* 22, no. 11: 999–1002. https://doi.org/10.1130/0091-7613(1994)022<>2.3.CO;2.

Orme, D. A., B. Carrapa, and P. Kapp. 2015. "Sedimentology, Provenance and Geochronology of the Upper Cretaceous–Lower Eocene Western Xigaze Forearc Basin, Southern Tibet." *Basin Research* 27: 387–411. https://doi.org/10.1111/bre.12080.

Orme, D. A., and A. K. Laskowski. 2016. "Basin Analysis of the Albian–Santonian Xigaze Forearc, Lazi Region, South-Central Tibet." *Journal of Sedimentary Research* 86: 894–913. https://doi.org/10.2110/jsr.2016.57.

Orme, D. A., N. Weis, K. D. Surpless, et al. 2025. "Age, Provenance, and Geochemical Relationships Amongst the Great Valley Group, Coast Range Ophiolite, and Franciscan Subduction Complex at Del Puerto Canyon, Central California." *Geological Society of America Bulletin* 137: 4659–4685. https://doi.org/10.1130/B38093.1.

Pan, G. T., Z. L. Chen, X. Z. Li, and Y. J. Yan. 1997. *Formation and Evolution of East Tethys Geological Structure*. Geological Publishing House. (in Chinese.).

Pullen, A., P. Kapp, G. E. Gehrels, J. D. Vervoort, and L. Ding. 2008. "Triassic Continental Subduction in Central Tibet and Mediterranean-Style Closure of the Paleo-Tethys Ocean." *Geology* 36, no. 5: 351–354. https://doi.org/10.1130/G24435A.1.

Qiu, Z. Y., S. Li, M. Dai, X. D. Cui, and M. Deng. 2024. "Geochemical Characteristics of Triassic Granites in the Songpan-Ganzi Orogenic Belt and Its Implication for Lithium Mineralization." *Acta Petrologica Sinica* 40, no. 12: 3876–3890. https://doi.org/10.18654/1000-0569/2024.12.05.

Reid, A., C. J. Wilson, L. Shun, N. Pearson, and E. Belousova. 2007. "Mesozoic Plutons of the Yidun Arc, SW China: U/pb Geochronology and hf Isotopic Signature." *Ore Geology Reviews* 31: 88–106. https://doi.org/10.1016/j.oregeorev.2004.11.003.

Reid, A. J., C. J. Wilson, and S. Liu. 2005. "Structural Evidence for the Permo-Triassic Tectonic Evolution of the Yidun Arc, Eastern Tibetan Plateau." *Journal of Structural Geology* 27, no. 1: 119–137. https://doi.org/10.1016/j.jsg.2004.06.011.

Reid, A. J., C. J. Wilson, D. Phillips, and S. Liu. 2005. "Mesozoic Cooling Across the Yidun Arc, Central-Eastern Tibetan Plateau: A Reconnaissance 40Ar/39Ar Study." *Tectonophysics* 398: 45–66. https://doi.org/10.1016/j.tecto.2005.01.002.

Richards, J. P. 2009. "Postsubduction Porphyry cu-Au and Epithermal au Deposits: Products of Remelting of Subduction-Modified Lithosphere." *Geology* 37, no. 3: 247–250. https://doi.org/10.1130/G25451A.1.

Roger, F., J. Malavieille, P. H. Leloup, S. Calassou, and Z. Xu. 2004. "Timing of Granite Emplacement and Cooling in the Songpan–Garze Fold Belt (Eastern Tibetan Plateau) With Tectonic Implications." *Journal of Asian Earth Sciences* 22: 465–481. https://doi.org/10.1016/j.jseaes.2003.09.004.

Solidum, R. U., P. R. Castillo, and J. W. Hawkins. 2003. "Geochemistry of Lavas From Negros Arc, West Central Philippines: Insights Into the Contribution From the Subducting Slab." *Geochemistry, Geophysics, Geosystems* 4: 1077. https://doi.org/10.1029/2003GC000513.

Sun, G., X. Hu, E. Garzanti, et al. 2023. "Pre-Eocene Arabia-Eurasia Collision: New Constraints From the Zagros Mountains (Amiran Basin, Iran)." *Geology* 51, no. 10: 941–946. https://doi.org/10.1130/G51321.1.

Surpless, K. D. 2015. "Geochemistry of the Great Valley Group: An Integrated Provenance Record." *International Geology Review* 57: 747–766. https://doi.org/10.1080/00206814.2014.943295.

Tang, Y., Y. D. Li, D. B. Wang, et al. 2025. "Chronological, Geochemical Characteristics and Tectonic Evolution Significance of the Sanyan Eclogites in the Jinsha River Suture Zone, Eastern Xizang." *Journal of Geomechanics* 31: 557–575. https://doi.org/10.12090/j.issn.1006-6616.2025053.

Tang, Y., A. Yin, X. Xu, K. An, and Y. Zhang. 2023. "Tectonic Evolution of the Triassic Songpan-Ganzi Basin as Constrained by a Synthesis of Multi-Proxy Provenance Data." *Basin Research* 35, no. 1: 28–60. https://doi.org/10.1111/bre.12703.

Tian, Z., C. Leng, J. Guo, X. Zhang, F. Tian, and R. Ma. 2023. "Early Paleozoic Tectonic Framework of the Yidun Terrane, Eastern Tibetan Plateau: Constraints From Detrital Zircon U-Pb-Hf Isotopic Compositions." *Acta Geologica Sinica* 97, no. 4: 1088–1105. (in Chinese with English abstract.).

Wang, B. Q., W. Wang, and M. F. Zhou. 2013. "Provenance and Tectonic Setting of the Triassic Yidun Group, the Yidun Terrane, Tibet." *Geoscience Frontiers* 4: 765–777. https://doi.org/10.1016/j.gsf.2013.02.004.

Wang, D. B., Y. Tang, L. Luo, et al. 2024. "Timing of Closure of the Jinshajiang Paleo-Tethys Ocean in Eastern Tibet: Constraints From the Early–Middle Triassic Unconformity and Collision-Related Igneous Rock in the Eastern Margin of Qamdo Block." *Acta Petrologica Sinica* 40: 3801–3816. https://doi.org/10.18654/1000-0569/2024.12.06.

Wang, E., K. Meng, Z. Su, et al. 2014. "Block Rotation: Tectonic Response of the Sichuan Basin to the Southeastward Growth of the Tibetan Plateau Along the Xianshuihe-Xiaojiang Fault." *Tectonics* 33: 686–718. https://doi.org/10.1002/2014TC003561.

Wang, Q., Z. X. Li, S. L. Chung, et al. 2011. "Late Triassic High-Mg Andesite/Dacite Suites From Northern Hohxil, North Tibet: Geochronology, Geochemical Characteristics, Petrogenetic Processes and Tectonic Implications." *Lithos* 126, no. 1–2: 54–67. https://doi.org/10.1016/j.lithos.2011.06.002.

Wang, X., I. Metcalfe, P. Jian, L. He, and C. Wang. 2000. "The Jinshajiang-Ailaoshan Suture Zone, China: Tectonostratigraphy, Age and Evolution." *Journal of Asian Earth Sciences* 18, no. 6: 675–690. https://doi.org/10.1016/S1367-9120(00)00039-0.

Weislogel, A., S. Graham, E. Chang, J. Wooden, and G. Gehrels. 2010. "Detrital Zircon Provenance From Three Turbidite Depocenters of the Middle-Upper Triassic Songpan-Ganzi Complex, Central China: Record of Collisional Tectonics, Erosional Exhumation, and Sediment Production." *Geological Society of America Bulletin* 122, no. 11–12: 2041–2062. https://doi.org/10.1130/B26606.1.

Weislogel, A. L. 2006. "The Sedimentary Record of Mesozoic Collisional Orogenesis, Central China: Geochemical, Geochronometric and Paleoenvironmental Constraints." Doctoral Dissertation, Stanford University, USA.

Weislogel, A. L., S. A. Graham, E. Z. Chang, J. L. Wooden, G. E. Gehrels, and H. Yang. 2006. "Detrital Zircon Provenance of the Late Triassic Songpan-Ganzi Complex: Sedimentary Record of Collision of the North and South China Blocks." *Geology* 34, no. 2: 97–100. https://doi.org/10.1130/G21929.1.

Wu, T., L. Xiao, S. A. Wilde, C. Q. Ma, and J. X. Zhou. 2017. "A Mixed Source for the Late Triassic Garzê-Daocheng Granitic Belt and Its Implications for the Tectonic Evolution of the Yidun Arc Belt, Eastern Tibetan Plateau." *Lithos* 288: 214–230. https://doi.org/10.1016/j.lithos.2017.07.013.

Xiao, L., H. F. Zhang, J. D. Clemens, et al. 2007. "Late Triassic Granitoids of the Eastern Margin of the Tibetan Plateau: Geochronology, Petrogenesis and Implications for Tectonic Evolution." *Lithos* 96: 436–452. https://doi.org/10.1016/j.lithos.2006.11.008.

Xu, Z., B. Zheng, W. Zhu, et al. 2024. "The Cimmeride Orogeny and the Genesis of the Songpan-Ganze "Lithium Deposit Chain"." *Acta Geologica Sinica* 98, no. 5: 1333–1357. https://doi.org/10.19762/j.cnki.dizhixuebao.2024108. (in Chinese with English abstract.).

Yan, H., Z. Xu, G. Li, B. Zheng, J. Gao, and X. Long. 2024. "Whole-Rock and Apatite Geochemistry of Late Triassic Plu–Nic Rocks in the Eastern Songpan-Ganzi Orogenic Belt: Petrogenesis and Implications for Tectonic Evolution." *Lithosphere* 2024, no. 1: lithosphere_2023_284. https://doi.org/10.2113/2024/lithosphere_2023_284.

Yang, K., W. G. Zhu, C. Li, et al. 2024. "Discovery of Mafic Dikes in Northeastern Tibet Plateau Belonging to the Emeishan Large Igneous Province: Implications for Paleocontinental Reconstruction and Mineral Exploration." *Gondwana Research* 136: 1–13. https://doi.org/10.1016/j.gr.2024.07.006.

Yu, G. M., S. D. Mao, Z. J. Zhou, G. Xie, and H. Q. Huang. 2024. "Late Paleozoic Tectonic Evolution of Ganzi-Litang Ocean in Sanjiang Region, Southwest China: Constraints From U-Pb Geochronology of Cumulate Gabbro in Litang Ophiolitic Mélange Belt." *Geological Bulletin of China* 43, no. 1: 61–75. http://dzhtb.cgs.cn/article/doi/10.12097/gbc.2022.01.023. (in Chinese with English abstract.).

Yuan, C., M. F. Zhou, M. Sun, et al. 2010. "Triassic Granitoids in the Eastern Songpan Ganzi Fold Belt, SW China: Magmatic Response – Geodynamics of the Deep Lithosphere." *Earth and Planetary Science Letters* 290: 481–492. https://doi.org/10.1016/j.epsl.2009.12.032.

Zhan, Q. Y., D. C. Zhu, Q. Wang, et al. 2020. "Source and Pressure Effects in the Genesis of the Late Triassic High Sr/Y Granites From the Songpan-Ganzi Fold Belt, Eastern Tibetan Plateau." *Lithos* 368: 105584. https://doi.org/10.1016/j.lithos.2020.105584.

Zhan, Q. Y., D. C. Zhu, Q. Wang, et al. 2021. "Imaging the Late Triassic Lithospheric Architecture of the Yidun Terrane, Eastern Tibetan Plateau: Observations and Interpretations." *Bulletin of the Geological Society of America* 133, no. 11–12: 2279–2290. https://doi.org/10.1130/B35778.1.

Zhu, D. C., Q. Wang, R. F. Weinberg, et al. 2022. "Interplay Between Oceanic Subduction and Continental Collision in Building Continental Crust." *Nature Communications* 13, no. 1: 7141. https://doi.org/10.1038/s41467-022-34826-0.

Zhu, D. C., Q. Wang, R. F. Weinberg, et al. 2023. "Continental Crustal Growth Processes Recorded in the Gangdese Batholith, Southern Tibet." *Annual Review of Earth and Planetary Sciences* 51, no. 1: 155–188. https://doi.org/10.1146/annurev-earth-032320-110452.

Zhu, D. C., Q. Wang, Q. Y. Zhan, and J. C. Xie. 2021. "Late Triassic Tectono-Magmatism of Northern Sanjiang and Associated Several Scientific Problems." *Sedimentary Geology and Tethyan Geology* 41, no. 2: 232–245. https://doi.org/10.19826/j.cnki.1009-3850.2021.03002. (in Chinese with English abstract.).

Zi, J. W., P. A. Cawood, W. M. Fan, et al. 2013. "Late Permian-Triassic Magmatic Evolution in the Jinshajiang Orogenic Belt, SW China and Implications for Orogenic Processes Following Closure of the Paleo-Tethys." *American Journal of Science* 313, no. 2: 81–112. https://doi.org/10.2475/02.2013.02.

Supporting Information

Additional supporting information can be found online in the Supporting Information section. **Figure S1:** Zircon U–Pb concordia diagrams of granites and volcanic rocks from the Zhongza terrane. **Figure S2:** Relative probability plots of concordant detrital zircon U–Pb ages of the Triassic turbidites from the Zhongza terrane in this study. **Figure S3:** Paleocurrent indicator orientation rose diagrams. **Table S1:** Compiled zircon U–Pb ages of magmatic rocks in the Songpan-Ganzi terrane and Zhongza terrane. **Table S2:** Sample information of published Palaeozoic detrital zircon U–Pb age dating and references from the eastern Tibetan Plateau. Published Palaeozoic detrital zircon U–Pb best ages with error from the sandstones in the eastern Tibetan Plateau. **Table S3:** Compiled whole-rock major- and trace-elements, zircon Hf, and whole-rock Sr-Nd isotopic data of Late Triassic intrusive and volcanic rocks in the Zhongza terrane. **Table S4:** Sandstone petrography data obtained by point-counting in thin sections according to the Gazzi-Dickinson method. **Table S5:** Detrital zircon U–Pb age (Ma) data from Triassic strata in the Zhongza terrane. **Table S6:** Previously published detrital zircon U–Pb age (Ma) data from Pre-Triassic strata in the Zhongza terrane, Songpan-Ganzi terrane, East Kunlun orogen, South China Block, North Qinling orogenic belt, South Qinling orogenic belt, North China Block, and Qiangtang terrane.